Inorganic Chemistry

COMMUNICATION

pubs.acs.org/IC

Ferromagnetic Exchange Couplings Showing a Chemical Trend in Cu−Ln−Cu Complexes (Ln = Gd, Tb, Dy, Ho, Er)

Takashi Shimada,[†] Atsushi Okazawa,[‡] Norimichi Kojima,[‡] Shunsuke Yoshii,[§] Hiroyuki Nojiri,[*,§] and Takayuki Ishida[*,†]

[†]Department of Engineering Science, The University of Electro-Communications, Chofu, Tokyo 182-8585, Japan

[‡]Department of Basic Science, Graduate School of Arts and Sciences, The University of Tokyo, Tokyo 182-8585, Japan

[§]Institute for Materials Research and CINTS, Tohoku University, Katahira, Sendai 980-8577, Japan

Supporting Information

ABSTRACT: Exchange couplings in isomorphous [$LnCu_2$] were evaluated by high-frequency electron paramagnetic resonance and magnetization studies. The exchange parameter J_{Ln-Cu} was decreased with an increase in the atomic number; J_{Ln-Cu}/k_B = 4.45(11), 2.27(6), 0.902(10), 0.334(3), and 0.136(8) K for Ln = Gd, Tb, Dy, Ho, and Er, respectively.

Heterometallic 4f−3d compounds have been intensively studied for the development of single-molecule magnets (SMMs),[1−3] where strong magnetic anisotropy and large spin are available from lanthanide (Ln) ions.[4] The exchange coupling between 4f and 3d spins is one of the most important parameters, and we have established a standard method to determine quantitatively the exchange couplings[5,6] by means of combined high-frequency electron paramagnetic resonance (HF-EPR) and pulsed-field magnetization techniques.[7] The outline is as follows:[8] (1) Ln ions are treated as Ising spins. (2) Energy levels of the spin states are defined by 4f−3d exchange coupling parameters (J_{Ln-M}) at zero field. (3) The Zeeman diagram is drawn, where level crossings take place. (4) Magnetization steps and EPR transitions are assigned. For ferromagnetic compounds like the present compounds, the magnetization curve will show a featureless increase. The variable-frequency EPR technique is a practically unique option to determine precisely a negative level-crossing field.

To exploit broad application of this method, we prepared linear trinuclear [$Ln^{III}Cu^{II}_2$] complexes and studied the 4f−3d magnetic couplings. After Fenton et al. reported the preparation of 2,6-bis(acetylaceto)pyridine[9] (abbreviated as H_2L hereafter), Shiga et al. developed the L_2-sandwiched Cu−Ln−Cu architecture showing at least five (pseudo)polymorphic types of $LnCu_2L_2(NO_3)_3(solv.)_n$.[10] We successfully prepared a completely isomorphous series of $[LnL_2(NO_3)_2\{Cu(CH_3OH)\}_2](NO_3)\cdot(CH_3OH)$ ([$LnCu_2$]) for heavy Ln ions [Ln = Gd (S_{Gd} = $^7/_2$ and g_{Gd} = 2), Tb (J_{Tb} = 6 and g_{Tb} = $^3/_2$), Dy (J_{Dy} = $^{15}/_2$ and g_{Dy} = $^4/_3$), Ho (J_{Ho} = 8 and g_{Ho} = $^5/_4$), Er (J_{Er} = $^{15}/_2$ and g_{Er} = $^6/_5$)].[11]

The molecular structures were determined by means of X-ray crystallographic analysis [Figure 1 for Ln = Tb and Figure S1 (Supporting Information) for other derivatives].[12] They crystallize in a triclinic $P\bar{1}$ space group with Z = 2. The whole molecule is crystallographically independent, but an inversion center is approximately assumed at the Ln ion. The ions are connected with double μ-oxo bridges.[11] The Ln−O distances as well as the cell volume indicate the ionic radius contraction in the order of the atomic number. Despite such a contraction, the geometrical change seems to be considerably small, and the variation of magnetic couplings can be attributed to the atomic character itself.

The Tb and Dy derivatives behaved as SMMs, as is clearly shown by magnetic hysteresis. The magnetization jumps were observed at 0.88 and 1.03 T for [$TbCu_2$] and 0.41 and 0.54 T for [$DyCu_2$] at 0.5 K (Figure 2), and their positions did not depend on the field scanning rate or temperature, being compatible with the quantum tunneling of magnetization (QTM). The dynamics were investigated by means of an alternating-current (ac) susceptibility technique, giving the following parameters from the Arrhenius equation:[13] $\ln(2\pi\nu) = -\ln(\tau_0) - E_a/k_BT$, where E_a (activation energy) = 14.2(5) K and τ_0 (preexponential factor) = 7.3×10^{-8} s for [$TbCu_2$] (Figure S3, Supporting Information). As for [$DyCu_2$], blocking takes place below 1.6 K, and the Arrhenius analysis is unavailable in our apparatus.

HF-EPR spectra of polycrystalline [$LnCu_2$] (Ln = Tb, Dy, Ho, Er) were collected in a wide frequency range between 95 and 405 GHz at 4.2 K (Figure 3). We found practically single series of absorptions shifted to a higher field with increasing frequency. The g values were around 2 from the slope of the frequency−field plot (dotted lines), being consistent with the Cu spin-flip signal satisfying a conventional EPR selection rule of $\Delta m_s = \pm 1$.

The line has a negative-field bias from the normal Zeeman effect. Because there is no single-ion-type anisotropy in Cu spins, the observed characteristic frequency−field relationship shows the presence of an internal exchange-bias field at the Cu site. As described for the simplest dinuclear Ln−M model,[8] ferro- and antiferromagnetic systems show negative and positive shifts of the Zeeman lines, respectively. The Ln ions are treated as Ising spins. The present trinuclear system should show major EPR absorption ascribable to the transition from the ground [Cu(↑)−Ln(↑)−Cu(↑)] state to the first excited [Cu(↑)−Ln(↑)−Cu(↓)] state. The Ising-type spin Hamiltonian (eq 1) is applied to the present system.

$$H = -J_{Ln-Cu}(J^z_{Ln}\cdot S_{Cu1} + J^z_{Ln}\cdot S_{Cu2}) + \mu_B H^z(g_{Ln}J^z_{Ln} + g_{Cu1}S_{Cu1} + g_{Cu2}S_{Cu2}) \quad (1)$$

Received: September 5, 2011
Published: October 03, 2011

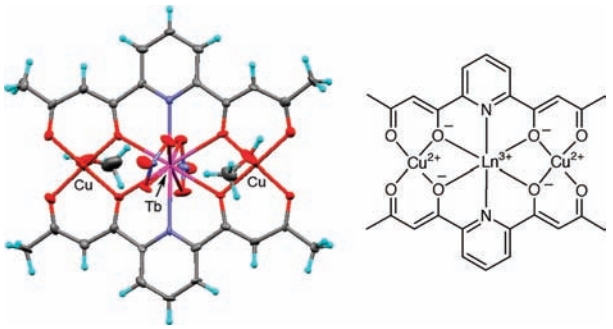

Figure 1. X-ray crystal structure of $[TbL_2(NO_3)_2\{Cu(CH_3OH)\}_2]^+$ with thermal ellipsoids at the 50% probability level for non-H atoms. The structural formula of the $[LnCu_2L_2]^{2+}$ plane is also shown.

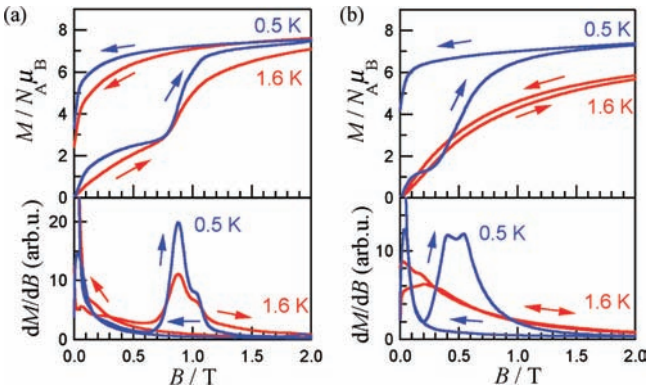

Figure 2. Pulsed-field magnetization at 1.6 and 0.5 K with a field sweep rate of 3×10^3 T s^{-1} for (a) $[TbCu_2]$ and (b) $[DyCu_2]$. The derivatives are also shown at the bottom.

The level-crossing field (B_C), together with the g factor, was determined from extrapolation in these plots (Figure 3). The energy gap (ΔE) between the ground and first excited states at zero field was converted directly from B_C, and J_{Ln-Cu} was derived according to the relation $\Delta E = -2J_{Ln-Cu}(J^z_{Ln} \cdot S_{Cu})$ from the first term of eq 1. To determine J_{Ln-Cu}, the value of J^z_{Ln} is required and actually estimated from the saturation magnetization (M_S; Figure 2 for instance), together with those reported for the closely related $[LnCu_2]$ compounds,[10] giving $J^z_{Ln} = 5$, $^{11}/_2$, 7, and $^{11}/_2$ for $[TbCu_2]$, $[DyCu_2]$, $[HoCu_2]$, and $[ErCu_2]$, respectively. However, incomplete field orientation of crystallites may give rise to an underestimation of M_S and J^z_{Ln}.

The energy diagrams help us to solve this problem (Figure 4). The level crossing due to the Cu spin flip occurs at P1 (−10.5 T) for $[TbCu_2]$, while other crossings are found at 1.02 T (P2) and 1.27 T (P3) with the maximal $J^z_{Tb} = 6$ (Figure 4a), which corresponds to the positions of two magnetization jumps observed around 1 T. These positions are sensitively shifted by J^z_{Ln}. The apparent J^z_{Tb} value of 5 would give higher crossing fields (1.20 and 1.56 T), and this assumption seems less likely. Similarly, for $[DyCu_2]$, the level crossings are found at −5.0, 0.46, and 0.56 T for $[DyCu_2]$ with $J^z_{Dy} = {}^{15}/_2$ (Figure 4b), being in good agreement with the two magnetization jump positions around 0.5 T. The value of $J^z_{Dy} = {}^{11}/_2$ is rejected because the resultant level-crossing fields (0.72 and 1.00 T) are unsatisfactory.

Thus, the maximal J^z_{Ln} is suggested in $[LnCu_2]$, and we obtained the exchange parameters as follows: $J_{Ln-Cu}/k_B = 2.27(6)$, 0.902(10), 0.334(3), and 0.136(8) K for Ln = Tb, Dy, Ho, and Er, respectively.[14]

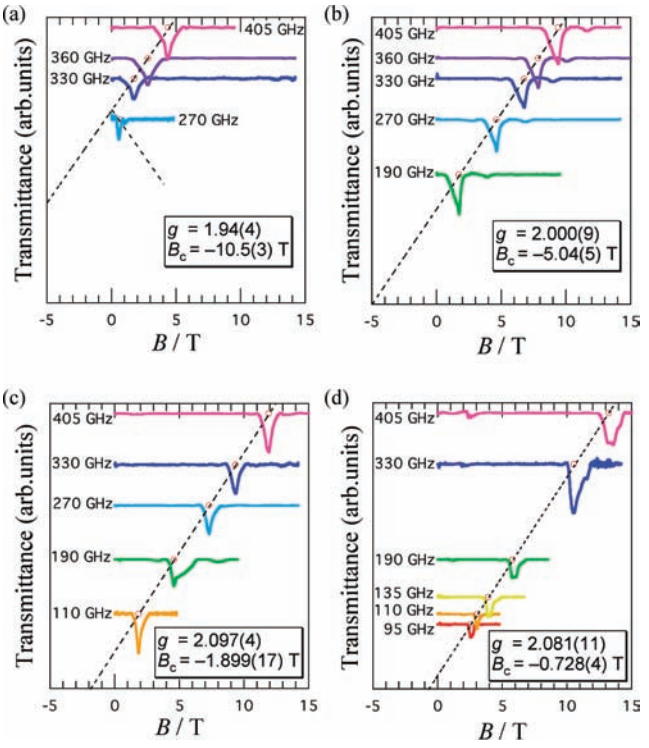

Figure 3. Selected HF-EPR spectra of $[LnCu_2]$ measured at 4.2 K [Ln = (a) Tb, (b) Dy, (c) Ho, and (d) Er]. The spectra are offset in a linear scale of the frequency. Dotted lines are drawn from the linear fitting in the frequency−field plot.

The HF-EPR technique gave no meaningful information on J_{Gd-Cu}. Instead, we measured the conventional magnetic susceptibility χ_m as a function of T from which J_{Gd-Cu} could easily be characterized thanks to the spin-only character of Gd^{3+} (Figures S4 and S5, Supporting Information). The $\chi_m T$ value monotonically increased upon cooling, and J_{Gd-Cu} was determined according to the van Vleck equation involving Heisenberg spins,[15] to afford $J_{Gd-Cu}/k_B = 4.45(11)$ K with $g_{avg} = 1.990(4)$.

We can compare J_{Ln-Cu} of various $[LnCu_2]$ in a highly quantitative manner for the first time (Figure 5). In general, the $\Delta(\chi T)$ vs T strategy[16] is available as an empirical measurement by use of isomorphous reference compounds with diamagnetic ions, where $\Delta(\chi T)$ is $(\chi T)_{sample} - (\chi T)_{reference}$. For the $[LnCu_2]$-type compounds, such $\Delta(\chi T)$ analysis suggested ferromagnetic couplings for Ln = Tb−Er,[10] but their magnitudes were unknown until now. The advantage of the present study is to determine J_{Ln-Cu} directly and precisely.

Another striking result of this work is the observation of a distinct chemical trend in J_{Ln-Cu}. Many ferromagnetic Gd−Cu compounds have been reported,[16−18] and Kahn et al. qualitatively explained the ferromagnetic couplings between Cu^{2+} and heavy Ln^{3+} ions.[18] From the present quantitative analysis, the interaction becomes weaker in the order Gd^{3+} to Er^{3+}. The nominal number of 4f electrons increases from 7 to 11 and, accordingly, the number of the unpaired 4f electrons decreases from 7 to 3. The exchange coupling would take place between the Cu $3d_{x^2-y^2}$ spin and the Ln 4f spin portion (S_{Ln}) and has no relation with the Ln angular contribution or magnetic anisotropy. Such an observation has also been reported for the di-[8] and

dx.doi.org/10.1021/ic201944s |Inorg. Chem. 2011, 50, 10555–10557

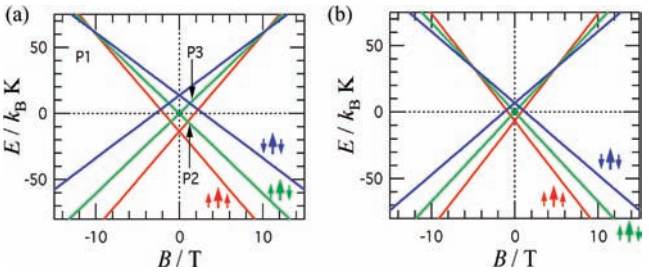

Figure 4. Energy levels of (a) [$TbCu_2$] and (b) [$DyCu_2$] in a ground-state manifold. The spin structures are indicated with small arrows.

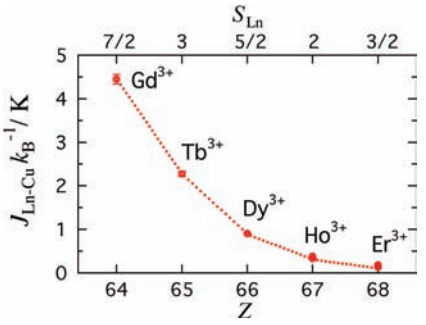

Figure 5. Plot of the 4f−3d exchange parameters in [$LnCu_2$] as a function of the atomic number (Z) and spin quantum number (S_{Ln}) for Ln^{3+}. A broken line is drawn for a guide to the eye.

tetranuclear systems.[6] The J_{Ln-Cu} chemical trend is thus generalized, regardless of the sign of J_{Ln-Cu}.

In summary, the magnetization measurements and HF-EPR spectroscopy are complementary methods for elucidation of the spin structures and energy diagrams for 4f−3d heteronuclear systems. When the 4f−3d specimen showed QTM, the step positions helped us to determine the J_{Ln-Cu} value.

■ ASSOCIATED CONTENT

Supporting Information. X-ray diffraction study (Figures S1 and S2) and CIF data for [$LnCu_2$] (Ln = Gd, Tb, Dy, Ho, Er), ac magnetic susceptibility results on [$TbCu_2$] (Figure S3), and HF-EPR results (Figure S4) and $\chi_m T$ vs T and M vs H plots for [$GdCu_2$] (Figure S5). This material is available free of charge via the Internet at http://pubs.acs.org.

■ AUTHOR INFORMATION

Corresponding Author

*E-mail: nojiri@imr.tohoku.ac.jp (H.N.), ishi@pc.uec.ac.jp (T.I.).

■ ACKNOWLEDGMENT

This work was partly supported by Grants-in-Aid for Scientific Research from MEXT, Japan, GCOE program: Materials Integration, and the Inter-University Cooperative Research Program of the Institute for Materials Research, Tohoku University, Sendai, Japan. Part of this work was performed at CINTS, Tohoku University.

■ REFERENCES

(1) Osa, S.; Kido, T.; Matsumoto, N.; Re, N.; Pochaba, A.; Mrozinski, J. *J. Am. Chem. Soc.* **2004**, *126*, 420.

(2) Mori, F.; Nyui, T.; Ishida, T.; Nogami, T.; Choi, K.-Y.; Nojiri, H. *J. Am. Chem. Soc.* **2006**, *128*, 1440. Ueki, S.; Ishida, T.; Nogami, T.; Choi, K.-Y.; Nojiri, H. *Chem. Phys. Lett.* **2007**, *440*, 263.

(3) Pointillart, F.; Bernot, K.; Sessoli, R.; Gatteschi, D. *Chem.—Eur. J.* **2007**, *13*, 1602.

(4) Ishikawa, N.; Sugita, M.; Ishikawa, T.; Koshihara, S.-y.; Kaizu, Y. *J. Am. Chem. Soc.* **2003**, *125*, 8694.

(5) Okazawa, A.; Nogami, T.; Nojiri, H.; Ishida, T. *Inorg. Chem.* **2008**, *47*, 9763. Okazawa, A.; Nogami, T.; Nojiri, H.; Ishida, T. *Inorg. Chem.* **2009**, *48*, 3292. Okazawa, A.; Watanabe, R.; Nezu, M.; Shimada, T.; Yoshii, S.; Nojiri, H.; Ishida, T. *Chem. Lett.* **2010**, *39*, 1331.

(6) Okazawa, A.; Nogami, T.; Nojiri, H.; Ishida, T. *Chem. Mater.* **2008**, *20*, 3110. Okazawa, A.; Watanabe, R.; Nojiri, H.; Nogami, T.; Ishida, T. *Polyhedron* **2009**, *28*, 1808.Okazawa, A.; Fujiwara, K.; Watanabe, R.; Kojima, N.; Yoshii, S.; Nojiri, H.; Ishida, T. *Polyhedron* **2011**, DOI:10.1016/j.poly.2011.03.007.

(7) Nojiri, H.; Ajiro, Y.; Asano, T.; Boucher, J.-P. *New J. Phys.* **2006**, *8*, 218. Nojiri, H.; Choi, K.-Y.; Kitamura, N. *J. Magn. Magn. Mater.* **2007**, *310*, 1468.

(8) Watanabe, R.; Fujiwara, K.; Okazawa, A.; Tanaka, G.; Yoshii, S.; Nojiri, H.; Ishida, T. *Chem. Commun.* **2011**, *47*, 2110.

(9) Fenton, D. E.; Tate, J. R.; Casellato, U.; Tamburini, S.; Vigato, P. A.; Vidali, M. *Inorg. Chim. Acta* **1984**, *83*, 23.

(10) Shiga, T.; Ohba, M.; Okawa, H. *Inorg. Chem.* **2004**, *43*, 4435.

(11) For a detailed synthetic procedure and structural description, see ref 10, where the present compounds were classified as type "B1". New compounds were characterized by means of elemental and IR spectroscopic analyses as follows. Calcd for [$GdCu_2$]: C, 32.95; H, 3.24; N, 6.63. Found: C, 32.87; H, 3.10; N, 6.63. Calcd for [$TbCu_2$]: C, 32.90; H, 3.24; N, 6.62. Found: C, 33.04; H, 3.20; N, 6.88. Calcd for [$DyCu_2$]: C, 32.79; H, 3.23; N, 6.59. Found: C, 32.76; H, 3.13; N, 6.80. Calcd for [$HoCu_2$]: C, 32.72; H, 3.22; N, 6.58. Found: C, 32.69; H, 3.13; N, 6.82. Calcd for [$ErCu_2$]: C, 32.65; H, 3.21; N, 6.56. Found: C, 32.44; H, 3.10; N, 6.89. The IR spectra (neat; attenuated total reflection) showed absorption bands at 934−938, 1005−1025, 1285−1288, 1465−1468, 1516−1520, 1610−1612, and 3500 (br) cm^{-1} regardless of the Ln ions involved.

(12) Selected crystallographic data collected with monochromated Mo Kα radiation at T = 100 K are as follows. [$GdCu_2$]: $C_{29}H_{34}Cu_2GdN_5O_{20}$, a = 9.678(7) Å, b = 13.758(10) Å, c = 14.041(16) Å, α = 94.757(19)°, β = 103.12(2)°, γ = 102.02(2)°, V = 1764(3) $Å^3$, $R(F)$ [$I > 2\sigma(I)$] = 0.0522. [$TbCu_2$]: $C_{29}H_{34}Cu_2N_5O_{20}Tb$, a = 9.680(2) Å, b = 13.740(3) Å, c = 14.019(3) Å, α = 94.732(4)°, β = 103.090(4)°, γ = 101.976(4)°, V = 1760.2(6) $Å^3$, $R(F)$ [$I > 2\sigma(I)$] = 0.0672. [$DyCu_2$]: $C_{29}H_{34}Cu_2DyN_5O_{20}$, a = 9.6764(16) Å, b = 13.737(2) Å, c = 14.024(3) Å, α = 94.745(3)°, β = 103.032(4)°, γ = 101.970(4)°, V = 1760.1(5) $Å^3$, $R(F)$ [$I > 2\sigma(I)$] = 0.0496. [$HoCu_2$]: $C_{29}H_{34}Cu_2HoN_5O_{20}$, a = 9.6464(16) Å, b = 13.697(3) Å, c = 13.994(3) Å, α = 94.829(4)°, β = 102.855(4)°, γ = 101.825(4)°, V = 1748.0(5) $Å^3$, $R(F)$ [$I > 2\sigma(I)$] = 0.0664. [$ErCu_2$]: $C_{29}H_{34}Cu_2ErN_5O_{20}$, a = 9.628(3) Å, b = 13.661(5) Å, c = 13.975(5) Å, α = 94.867(16)°, β = 102.858(15)°, γ = 101.758(15)°, V = 1738.0(10) $Å^3$, $R(F)$ [$I > 2\sigma(I)$] = 0.0436. See also Figures S1 and S2 and CIF files in the Supporting Information.

(13) Gatteschi, D.; Sessoli, R. *Angew. Chem., Int. Ed.* **2003**, *42*, 268.

(14) The possibility of J^z_{Ho} = 7 or J^z_{Er} = $^{11}/_2$ cannot be completely eliminated, which afforded J_{Ho-Cu}/k_B = 0.382(5) K and J_{Er-Cu}/k_B = 0.185(2) K. These data points are superposed in Figure 5.

(15) Costes, J.-P.; Dahan, F.; Dupuis, A. *Inorg. Chem.* **2000**, *39*, 5994.

(16) Kahn, M. L.; Mathoniere, C.; Kahn, O. *Inorg. Chem.* **1999**, *38*, 3692.

(17) Bencini, A.; Benelli, C.; Caneschi, A.; Carlin, R. L.; Dei, A.; Gatteschi, D. *J. Am. Chem. Soc.* **1985**, *107*, 8128. Matsumoto, N.; Sakamoto, M.; Tamaki, H.; Okawa, H.; Kida, S. *Chem. Lett.* **1990**, 853. Guillow, O.; Bergerat, P.; Kahn, O.; Bakalbassis, E.; Boubekeur, K.; Batail, P.; Guillot, M. *Inorg. Chem.* **1992**, *31*, 110.

(18) Andruh, M.; Ramade, I.; Codjovi, E.; Guillou, O.; Kahn, O.; Trombe, J. C. *J. Am. Chem. Soc.* **1993**, *115*, 1822.